THE ASTROPHYSICAL JOURNAL, 438:908–916, 1995 January 10

THE PULSATION INDEX, EFFECTIVE TEMPERATURE, AND THICKNESS OF THE HYDROGEN LAYER IN THE PULSATING DA WHITE DWARF G117-B15A[1]

E. L. ROBINSON,[2] T. M. MAILLOUX,[2] E. ZHANG,[2] D. KOESTER,[3] R. F. STIENING,[4] R. C. BLESS,[5]
J. W. PERCIVAL,[5] M. J. TAYLOR,[5] AND G. W. VAN CITTERS[6]
Received 1994 May 11; accepted 1994 July 18

ABSTRACT

We have measured the amplitude of the 215 s pulsation of the pulsating DA white dwarf, or ZZ Ceti star, G117-B15A in six passbands with effective wavelengths from 1570 to 6730 Å. We find that the index of the pulsation is $\ell = 1$ with a high degree of confidence, the first unambiguous determination of ℓ for a pulsation of a ZZ Ceti star. We also find that log g and $T_{\rm eff}$ are tightly correlated for model atmospheres that fit the data, such that at log $g = 7.5$ the temperature is 11,750 K and at log $g = 8.0$ the temperature is 12,375 K. Adopting log $g = 7.97 \pm 0.06$ from published observations of the optical spectrum of G117-B15A, the correlation yields $T_{\rm eff} = 12{,}375 \pm 125$ K. This temperature is free of flux calibration errors and should be substantially more reliable than temperatures derived fro *IUE* spectra. Since G117-B15A is thought to lie close to the blue edge of the ZZ Ceti instability strip, this low temperature also implies a low temperature for the blue edge.

Using pulsation models calculated by Fontaine et al. (1992) and Bradley (1994), we find that the mass of the hydrogen layer in G117-B15A lies between $1.0 \times 10^{-6}\ M_\odot$ (for $k = 1$) and $8 \times 10^{-5}\ M_\odot$ (for $k = 2$). This range of masses is (barely) consistent with the masses predicted by recent models for the ejection of planetary nebulae, (8–13) $\times\ 10^{-5}\ M_\odot$. The mass is too large to be consistent with models invoking thin hydrogen layers to explain the spectral evolution of white dwarfs.

Subject headings: stars: individual (G117-B15A) — stars: oscillations — white dwarfs

1. INTRODUCTION

There are three groups of pulsating degenerate stars: the ZZ Ceti stars, which are DA white dwarfs with temperatures near 12,000 K; the pulsating DB white dwarfs, which have temperatures near 23,000 K; and the pulsating PG 1159−035 stars, also known as the GW Vir stars, which are pre–white dwarfs and have temperatures greater than 100,000 K. All three types are pulsating in the nonradial g-modes, all have periods between ~100 and ~1000 s, and all are multiperiodic (for a review see Winget 1988).

Observations of the pulsating white dwarfs can yield a detailed picture of their sturcture and evolution. If enough pulsation modes are excited and if the pulsation modes can be identified, the pulsation periods yield a star's mechanical properties, such as its total mass and the masses of its chemical-composition layers (see Kawaler & Hansen 1989). These mechanical properties can be compared directly to theories of the formation of white dwarfs through the ejection of planetary nebulae (Iben & MacDonald 1986), and to theories for the spectral evolution of white dwarfs (Fontaine & Wesemael 1991; D'Antona & Mazzitelli 1991). Furthermore, the periods of g-mode pulsations are sensitive to the thermal properties of the white dwarfs. The periods depend on the temperature of the white dwarf, and the rates of change of the periods yield the rate at which the white dwarf cools, which places limits on the composition of its core. The conversion of the white dwarf luminosity function into a constraint on the age and evolution of stars in the Galactic disk also requires the cooling rate (Wood 1992).

The pulsation modes must be individually identified to fully realize this potential. The modes are identified by the integer indices (ℓ, m, k), where ℓ and m are the indices of the spherical harmonics and give the number and distribution of pulsation nodes across the surface of the star, and k is the number of nodes in the radial direction.

Mode identification is a difficult problem. The general method has been to match observed pulsation periods to theoretical periods calculated using stellar structure and pulsation codes. Since there are many free parameters in these codes, the fits are ambiguous unless many pulsations are simultaneously excited in the star. The two stars with the most convincing mode identifications, PG 1159−035 and the DB white dwarf GD 358, have rich pulsation spectra, but, even so, the pulsations were only partially identified (Kawaler & Bradley 1994; Winget et al. 1994). Furthermore, when dealing with codes as sophisticated as those for calculating stellar structure and pulsation, questions concerning accuracy and uniqueness cannot be ignored. It is, therefore, important to determine pulsation indices in ways that do not depend on the details of the structure and pulsation calculations.

Mode identification for the ZZ Ceti stars presents special problems because none of the ZZ Ceti stars whose light curves have been decomposed into their constituent pulsations have enough large-amplitude pulsations to allow an unambiguous fit to the models. Clemens (1993) attempted to solve this

[1] Based in part on observations with the *Hubble Space Telescope* obtained at the Space Telescope Science Institute, which is operated by the Association of Universities for Research in Astronomy, Inc., under NASA contract NAS 5-26555.
[2] Department of Astronomy and McDonald Observatory, University of Texas, Austin, TX 78712.
[3] Institut für Theoretische Physik und Sternwarte, Universität Kiel, Olshausenstrasse 40, D-24098, Kiel, Germany.
[4] SSC Laboratory, 2550 Beckleymeade Avenue, Dallas, TX 75237.
[5] Department of Astronomy and Space Astronomy Laboratory, University of Wisconsin, Madison, WI 53706.
[6] Division of Astronomical Sciences, National Science Foundation, Washington, DC 20550, and Department of Aerospace Engineering, US Naval Academy, Annapolis, MD 21402.

problem by assuming that all DA white dwarfs are similar in structure and that one can construct a mean pulsation spectrum by adding the spectra of individual white dwarfs. There was, however, a 10%–20% probability that the pattern he found in the mean spectrum occurred by chance. Brassard et al. (1993) and Fontaine & Brassard (1994) have attempted to solve the problem by obtaining higher quality data in order to find more pulsation modes in individual stars. This method is promising, but more data are nceessary to confirm the reality of the weak mode splitting on which their results so far have relied. It is notable, however, that Clemens (1993), Brassard et al. (1993), and Fontaine & Brassard (1994) do assign the same pulsation index as we do to the main pulsation of G117-B15A, the subject of this paper.

In this paper we report multicolor, high-speed photometry of the ZZ Ceti star G117-B15A (= WD 0921 + 354 = RY LMi), including ultraviolet photometry with the *Hubble Space Telescope*. First found to be a variable by McGraw & Robinson (1976), its light curve was decomposed into its constituent pulsations by Kepler et al. (1982). The light curve is dominated by a single pulsation with a period of 215 s and an amplitude in white light near 2.2%. In addition, there is a pair of pulsations with periods of 271 and 304 s and amplitudes near 0.7%, and many weak pulsations with periods between 72 and 302 s (Brassard et al. 1993). The pulsation at 215 s is extraordinarily stable, the most recent measurement yielding $\dot{P} = (3.2 \pm 2.8) \times 10^{-15}$ s s^{-1} for the rate of change of its period (Kepler 1993). We show here that the amplitude of the 215 s pulsation at ultraviolet wavelengths constrains it to have an index $\ell = 1$. Our method does not depend on the details of pulsation theory or on the white dwarf structure, and in this sense it is model independent. This is the first unambiguous and model-independent determination of ℓ for a ZZ Ceti star.

2. THE OBSERVATIONS

We observed G117-B15A with the high-speed photometer on the *Hubble Space Telescope* (*HST*) six times in 1993 November, twice with the F145M filter, and four times with the F184W filter (Bless et al. 1994). The normalized response functions of the filters are shown in Figure 1, and their full widths at half-maximum and effective wavelengths are given in Table 1. For each observation the integration time was 0.05 s and the total time observed was 2688 s. The only data reduction necessary for the present experiment was to subtract a small contribution from background ($\sim$0.17 counts s^{-1}). All times have been converted to Terrestrial Dynamical Time, expressed as a Julian Date, and then converted to times of arrival at the barycenter of the solar system to give Barycentric Julian Dynamical Date (BJDD). The run names, filters, and Julian Dates of the observations are given in Table 2.

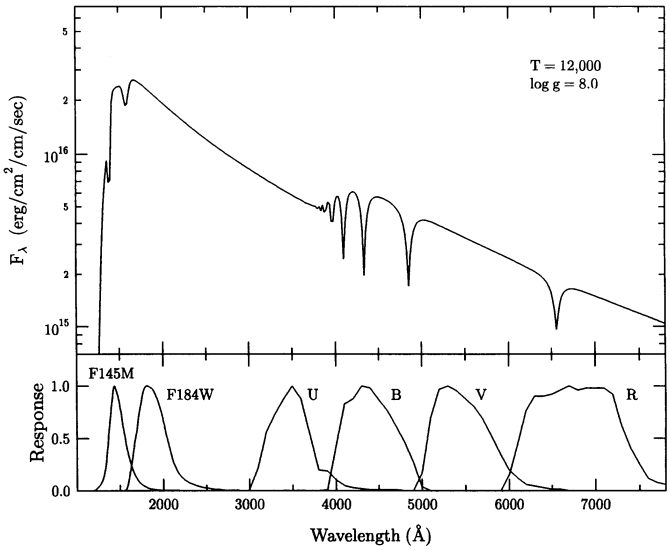

FIG. 1.—Shown in the lower panel are the response functions of the six filters normalized to 1.0 at the peaks of their responses. For comparison the upper panel shows the theoretical spectrum of a DA white dwarf with $T_{\rm eff}$ = 12,000 K and log g = 8.0.

The F184W light curve of G117-B15A is shown in Figure 2, and the F145M light curve is shown in Figure 3. The typical photon detection rates from G117-B15A were 2.2 counts s^{-1} through the F145M filter and 35.0 counts s^{-1} through the F184W filter. The 215 s pulsation has a mean amplitude of 4.8% ± 0.3% in the F184W light curve and is clearly visible, but it is not clearly visible in the F145M light curve even though its amplitude is much larger there, 10.4% ± 0.9%, because of the lower photon count rate and consequently higher photon count noise in that filter. Figures 4 and 5 show the power spectra of the light curves in Figures 2 and 3. Both power spectra have a strong feature near 0.00465 Hz produced by the 215 s pulsation; the power spectrum of the F184W light curve also shows a weaker feature near 0.0035 Hz produced by the pair of pulsations at 271 and 304 s. The amplitude of the feature near 0.0035 Hz is variable from observation to observation, presumably because of beating between the two unresolved pulsations. None of the other features in the power spectra are significant. The upper limit to the amplitude of any other pulsation in the F184W light curve is 2%.

We extracted amplitudes and times of pulse maximum for the 215 s pulsation by fitting a sine curve to each of the six light curves. The semiamplitudes and times of maxima are given in Table 2. The semiamplitude in each filter is given as a percentage of the mean flux from G117-B15A in that filter, thus allow-

TABLE 1

PROPERTIES OF FILTERS USED TO OBSERVE G117-B15A

Filter	$\lambda_{\rm eff}$ (Å)	FWHM (Å)
F145M.....	1570	215
F184W.....	1920	360
U	3480	520
B	4410	700
V	5450	760
R	6730	1260

TABLE 2

OBSERVED AMPLITUDES AND PHASES OF THE 215 s PULSATION THROUGH THE F145M AND F184W FILTERS

Run Name	Filter	BJDD Pulse Maximum (2,449,290.0+)	Semiamplitude (%)
v1m00403t.....	F184W	4.21426 (±5)	5.1 ± 0.5
v1m00404t.....	F184W	4.29390 (±5)	5.0 ± 0.5
v1m00103t.....	F145M	5.43958 (±7)	10.4 ± 1.3
v1m00104t.....	F145M	5.49439 (±8)	10.3 ± 1.3
v1m00303t.....	F184W	8.23929 (±5)	4.7 ± 0.5
v1m00304t.....	F184W	8.30404 (±5)	4.3 ± 0.5

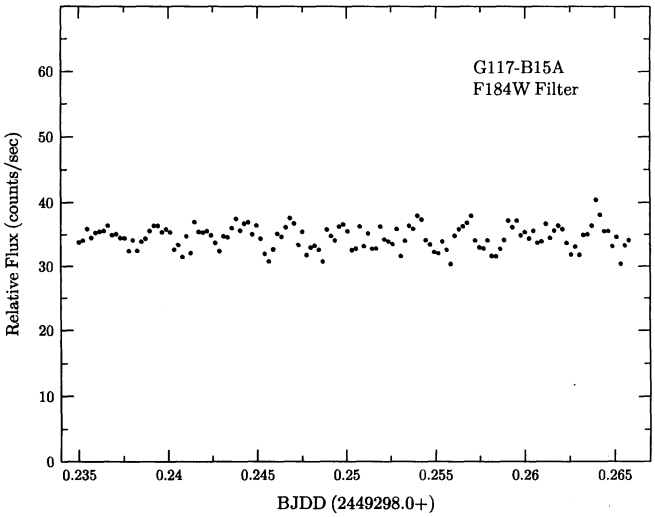

FIG. 2.—Ultraviolet light curve of G117-B15A through the F184W filter during run v1m00304t. The light curve has been rebinned to 20 s per point. The 215 s pulsation, which had an amplitude of 4.3% ± 0.5% during this run, is clearly present in the light curve.

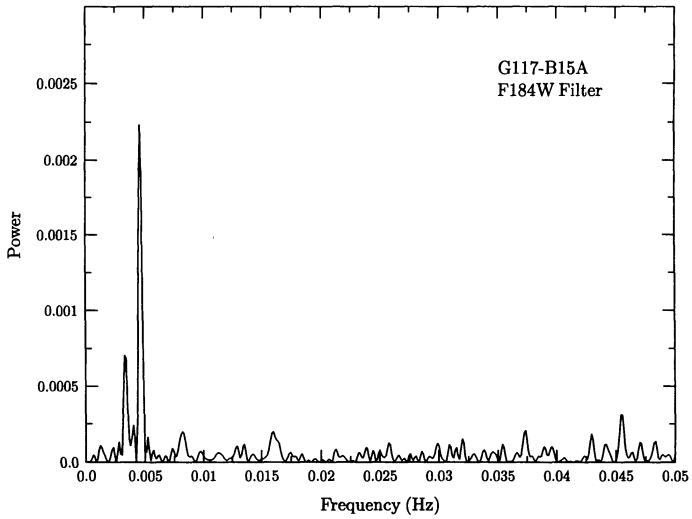

FIG. 4.—Low-frequency portion of the power spectrum of light curve v1m00304t, shown in Fig. 2. The only significant features are at frequencies of 0.00465 Hz, corresponding to the 215 s pulsation, and at 0.0035 Hz, corresponding to an unresolved pair of pulsations at 271.0 and 304.4 s.

ing us to bypass the difficult issues of calibration, centering of the star in the aperture of the high-speed photometer, interstellar reddening, and so on.

The ground-based photometry of G117-B15A was obtained with the Stiening high-speed photometer on the 2.1 m telescope at McDonald Observatory on five nights in 1993 February (see Zhang et al. 1991). The run names and Julian Dates of the observations are given in Table 3. The Stiening photometer measures fluxes in four passbands simultaneously. The response functions of the passbands are also shown in Figure 1, and their effective wavelengths and full widths at half-maximum are listed in Table 1. We call the four passbands *U*, *B*, *V*, and *R*, but they are different from and should not be confused with the Johnson *UBVR* filters. The data were reduced by subtracting the sky background and then roughly correcting for atmospheric extinction. Examples of the optical light curve of G117-B15A have already been published by McGraw & Robinson (1976), Kepler et al. (1982), and Fontaine & Brassard (1994).

The amplitudes and times of pulse maxima were extracted from the *UBVR* light curves in the same way as from the *HST* light curves. The semiamplitudes and times of maxima are given in Table 3, where the semiamplitudes are again given as a percentage of the mean flux. A clock error during run 466 prevented us from finding the absolute time of arrival of the pulses during the run, but the measued amplitues of the pulses are unaffected. Also, the sensitivity of the *V* detector drifted by a few percent during the observations, but the timescale of the drift was several hours, so the measurement of the fractional amplitude of the 215 s pulsation was not affected.

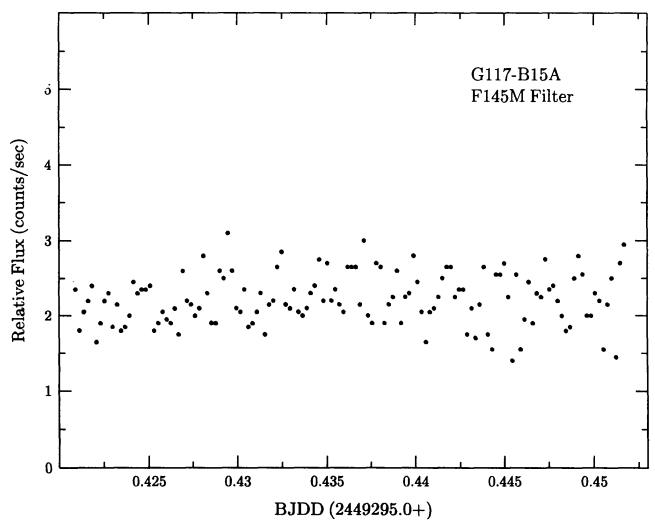

FIG. 3.—Ultraviolet light curve of G117-B15A through the F145M filter during run v1m00103t. The light curve has been rebinned to 20 s per point. Because of the low photon count rate, the 215 s pulsation is not obvious in the light curve, but a power spectrum of the light curve (see Fig. 5) shows that the pulsation is present and has an amplitude of 10.4% ± 1.3%.

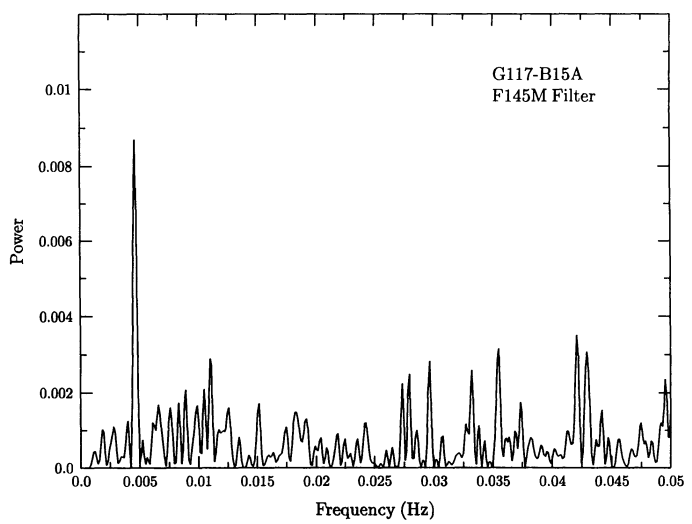

FIG. 5.—Low-frequency portion of the power spectrum of light curve v1m00103t, shown in Fig. 3. The only significant feature is at a frequency of 0.00465 Hz, corresponding to the 215 s pulsation.

TABLE 3

OBSERVED AMPLITUDES AND PHASES OF THE 215 s PULSATION THROUGH THE *U*, *B*, *V*, AND *R* FILTERS

RUN	BJDD PULSE MAXIMUM (2,449,000.0+)	SEMIAMPLITUDE (%)			
		U	*B*	*V*	*R*
460.....	36.80926 (±1)	2.26 ± 0.07	2.09 ± 0.07	1.74 ± 0.06	1.27 ± 0.10
465.....	38.67730 (±1)	2.22 ± 0.11	2.07 ± 0.11	1.84 ± 0.08	1.35 ± 0.21
466.....	...	2.46 ± 0.11	2.08 ± 0.11	1.86 ± 0.08	1.53 ± 0.21
467.....	40.68731 (±2)	2.16 ± 0.15	2.20 ± 0.15	...	1.28 ± 0.21
468.....	41.61636 (±2)	2.63 ± 0.15	2.46 ± 0.15	1.98 ± 0.12	1.68 ± 0.21

The weighted mean amplitudes of the 215 s pulsation in all the filters are given in column (2) of Table 4. Since the theory of nonradial pulsations in DA white dwarfs is not yet able to predict the amplitudes of the pulsations, we have normalized the amplitudes to the amplitude in the *V* band. The normalized amplitudes are given in column (3) of the table.

Because the *HST* and ground-based observations of G117-B15A were separated by more than 250 days, we must use the pulsation emphemeris to compare the times of arrival in the two data sets. S. O. Kepler (1994, private communication) has kindly supplied us with a recent update (see the footnote to our Table 4). Column (4) of Table 4 gives the mean values of the observed minus calculated ($O-C$) times of pulse maximum for the F145M, F184W, and *B* filters according to the recent ephemeris for G117-B15A given by Kepler (1993). The $O-C$ values are systematically early compared to the most recent ephemeris, but the observed times of arrival in the three filters are the same to within the observational uncertainty. The $O-C$ times for the remaining optical filters are nearly the same as that of the *B* filter, but because of the way the Stiening photometer takes data, timing errors in the four optical light curves are highly correlated and the remaining light curves give no extra timing information.

3. THE PHOTOMETRIC VARIATIONS OF *g*-MODE PULSATIONS

The theoretical spectral variations of low-amplitude *g*-mode pulsations in DA white dwarfs have been discussed by Robinson, Kepler, & Nather (1982, hereafter RKN). The effects of nonlinearities in temperature, which become important at higher amplitudes, have been discussed by Brassard, Wesemael, & Fontaine (1987) and Fontaine & Brassard (1994). The distance between the center of the white dwarf and any point on its surface varies by only a few parts in 10^{-5} for the typical observed luminosity variations. The geomtric distortions of the white dwarfs and the changes in their surface gravity due to changes in geometry are, therefore, too small to measure. The dominant effect of a pulsation is to create patches of higher and lower effective temperature on the surface of the white dwarf. For low-amplitude pulsations, the distribution of light across the surface is described by the spherical harmonics, where the distribution for any specific pulsation mode is described by a single spherical harmonic. A distant observer sees an average over these bright and dark patches. The pulsation periods are highly degenerate for spherical white dwarfs, but in real white dwarfs the degeneracy is removed by rotation or magnetic fields. Thus, the amplitude of the light variation at a particular period is the amplitude of the spherical harmonic corresponding to that pulsation averaged over the visible surface of the white dwarf.

TABLE 4

MEAN AMPLITUDES AND PHASES OF THE 215 s PULSATION

FILTER (1)	MEAN SEMIAMPLITUDE (%) (2)	NORMALIZED MEAN SEMIAMPLITUDE (3)	$O-C$[a] (s) (4)
F145M.....	10.4 ± 0.9	5.7 ± 0.5	−10.8 ± 4.3
F184W.....	4.8 ± 0.3	2.63 ± 0.17	−2.1 ± 2.1
U	2.32 ± 0.05	1.27 ± 0.04	...
B	2.13 ± 0.05	1.17 ± 0.04	−4.3 ± 0.6
V	1.82 ± 0.04	1.00	...
R	1.37 ± 0.08	0.75 ± 0.05	...

[a] $O-C$ calculated with respect to the quadratic ephemeris E_0 = BJDD 2,442,397.917525, P = 215.19738926 s, $\dot{P} = 3.2 \times 10^{-15}$ s s^{-1} (S. O. Kepler 1994, private communication).

With two important exceptions, we can use the framework developed by RKN to discuss our new observations. The exceptions are the following: (1) RKN calculated monochromatic flux variations. Since our observations were obtained through broadband filters, we must calculate the weighted average of the variations over the response function of our system. (2) RKN assumed that the limb darkening varied slowly with wavelength and could be approximated by a linear limb-darkening law. Neither of thse assumptions is correct at ultraviolet wavelengths, so we must allow for a more complicated limb-darkening law.

The weighted average over the filter bandpasses is easily incorporated in the calculation. If the observed time-averaged spectrum of the white dwarf is F_λ in ergs cm^{-2} s^{-1} Å^{-1} and the amplitude of the change in the spectrum due to pulsations is ΔF_λ, the fractional amplitude of the variations at wavelength λ is $\Delta F_\lambda / F_\lambda$. If the light curve of the white dwarf is measured through a broadband filter *i*, so that the response function for the entire system is $R_i(\lambda)$, the observed fractional amplitude of the variation, A_i, will be the weighted average

$$A_i = \frac{\int (\Delta F_\lambda / F_\lambda) \lambda F_\lambda R_i \, d\lambda}{\int \lambda F_\lambda R_i \, d\lambda} = \frac{\int \Delta F_\lambda \lambda R_i \, d\lambda}{\int F_\lambda \lambda R_i \, d\lambda} , \quad (1)$$

where the weighting function $\lambda F_\lambda R_i$ is proportional to the number of detected photons per unit wavelength in the unperturbed spectrum.

Allowance for a more complicated limb-darkening law produces a slight simplification in the formalism of RKN. The stellar spectra are given as sub–observer intensities at each wavelength plus a table of limb darkenings for several values of $\mu = \cos\theta$ at each wavelength. Equations (15) in RKN become

$$f_{0\lambda} = I_{0\lambda} h_\lambda(\mu) , \quad (2a)$$

$$\Delta f_\lambda = \epsilon I_{0\lambda} h_\lambda(\mu) \left(\frac{1}{I_{0\lambda}} \frac{\partial I_{0\lambda}}{\partial T} \right) \left(R_0 \frac{\delta T}{\delta r} \right) \xi_r , \quad (2b)$$

where $F_x c_x$ in that paper has been replaced by $I_{0\lambda}$, the sub–observer intensity, and the linear limb-darkening law $(1 - u_x + u_x \cos\theta)$ has been replaced by the arbitrary limb-darkening law $h_\lambda(\mu)$. R_0 is the unperturbed radius of the white dwarf, ξ_r is a spherical harmonic, and ϵ is the perturbation in the radius r. Equations (17) in RKN can no longer be integrated analytically over μ, and we leave them in the form

$$F_\lambda = 2\pi R_0^2 I_{0\lambda} \int h_\lambda(\mu)\mu\, d\mu\,, \tag{3a}$$

$$\Delta F_\lambda = 2\pi R_0^2 I_{0\lambda} \epsilon k_{\ell m} \left(\frac{1}{I_{0\lambda}}\frac{\partial I_{0\lambda}}{\partial T}\right)\left(R_0 \frac{\delta T}{\delta r}\right) \times \int h_\lambda(\mu) P_\ell(\mu)\mu\, d\mu\,, \tag{3b}$$

where $k_{\ell m}$ is a constant that depends on the orientation of the pulsation axis and the phase of the pulsation (see eq. [16b] in RKN), $P_\ell(\mu)$ is the Legendre polynomial of degree ℓ, and the integrals are evaluated between $\mu = 0$ and $\mu = 1$.

All factors in equation (3) that are independent of wavelength are irrelevant to the present observation, and so we have

$$F_\lambda \propto I_{0\lambda} \int h_\lambda(\mu)\mu\, d\mu\,, \tag{4a}$$

$$\Delta F_\lambda \propto I_{0\lambda}\left(\frac{1}{I_{0\lambda}}\frac{\partial I_{0\lambda}}{\partial T}\right) \int h_\lambda(\mu) P_\ell(\mu)\mu\, d\mu\,. \tag{4b}$$

For time-resolved spectrophotometry, equation (4) is the final result and the integration over the bandpass need not be performed.

It should be noted that equation (4) is true whenever the geometry at the surface is given by a spherical harmonic and the luminosity variations are due only to temperature variations. Thus the equation does not depend on the details of the pulsation theory or on the white dwarf structure, and in this sense it is model independent. Also, since equation (4) is independent of m, it is valid for unresolved blends of pulsations with the same ℓ but different m.

The theoretical spectra for DA white dwarfs are improved versions of the spectra described in Koester, Schulz, & Weidemann (1979) and Jordan & Koester (1986). The spectrum for $T = 12{,}000$ K, $\log g = 8.0$, and a pure hydrogen composition is shown in the upper panel of Figure 1. Lyα satellite absorption from the H_2^+ quasi-molecule and resonance broadening of Lyα by the H_2 quasi-molecule have been included in the opacities and produce the broad absorption features at 1400 and 1600 Å, respectively. The features fall within the passbands of the two ultraviolet filters. We calculated a grid of atmospheres with $\log g = 7.5$, 8.0, and 8.5, and $T_{\rm eff}$ running from 10,000 to 13,750 K in steps of 250 K, and we tabulated the limb darkening at six values of μ for each wavelength in each spectrum.

Figure 6 shows the intermediate result $\Delta F_\lambda/F_\lambda$ calculated for $T = 12{,}000$ K and $\log g = 8.0$, and for pulsation indices $\ell = 1$–4. The observed amplitudes of the pulsations in G117-B15A have also been placed on the graph, although only for comparison; the models cannot be fitted to the data quantitatively until the theoretical fluxes have been averaged over the filter responses.

The theoretical amplitudes are all much higher at ultraviolet wavelengths than at visual wavelengths because the ultraviolet wavelengths are near the peak or on the exponential tail of the spectral distributions (see Fig. 1), where variations in temperature produce a large change in flux. In addition, the amplitudes of the pulsations at ultraviolet wavelengths depend on the pulsation index. The source of the dependence is wavelength-dependent limb darkening. The observed amplitude of a nonradial pulsation is an average over all the bright and dark patches in view; for pulsations with high values of ℓ, there can be many bright and dark patches in view and considerable cancellation, reducing the observed amplitude greatly. The effect of limb darkening is to block off the limb of the white dwarf, so that less of the surface of the white dwarf is visible, fewer bright and dark patches are visible, and, consequently, there is less cancellation. At visual wavelengths the limb darkening is relatively small, so the amplitudes of pulsations with high ℓ are greatly reduced. At ultraviolet wavelength the limb darkening is large, so the amplitudes of pulsations with high ℓ suffer less cancellation and remain larger.

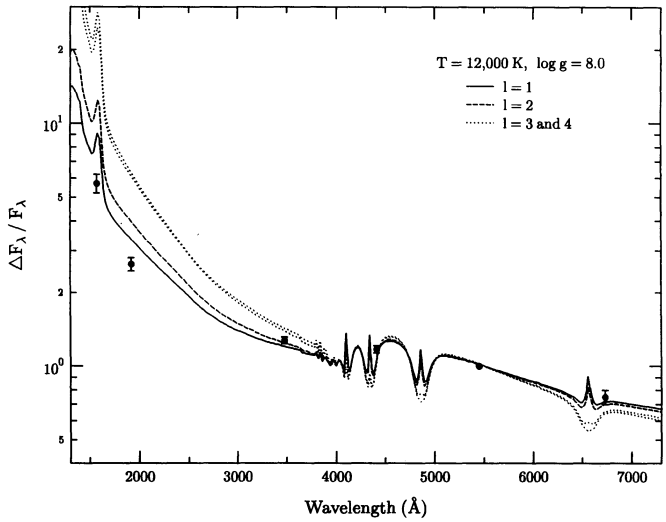

FIG. 6.—Intermediate result $\Delta F_\lambda/F_\lambda$ calculated for $T = 12{,}000$ K and $\log g = 8.0$, and for pulsation indices $\ell = 1$–4. The observed amplitudes of the pulsations in G117-B15A have also been placed on the graph, although only for comparison; the models cannot be fitted to the data quantitatively until the theoretical fluxes have been averaged over the filter responses.

Figure 7 shows the theoretical amplitudes of $\ell = 1$–4, nonradial g-mode pulsations in DA white dwarfs averaged over the response functions of the F145M, F184W, U, B, V, and R filters. The amplitudes have been calculated for a model with $T = 12{,}500$ K and $\log g = 8.0$, and have been normalized so that the amplitude through the V filter is 1.0. The observed amplitudes, also normalized have been superposed on the theoretical amplitudes. The $\ell = 1$ model is close to the best-fit model found in the next section.

4. A BAYESIAN DETERMINATION OF THE PULSATION INDEX l

We are given a set of observed amplitudes and standard deviations (a, σ) for the 215 s pulsation of G117-B15A, and a grid of theoretical amplitudes as a function of the temperature T, gravity g, and pulsation index ℓ. We ask which model best fits the data.

Figure 7 compares the theoretical and observed amplitudes of the pulsations for $\ell = 1$–4. The relatively low amplitudes of the pulsations observed through the two *HST* filters conclusively eliminate all values of ℓ greater than 2. We can also eliminate $\ell = 0$ because radial pulsation modes cannot have

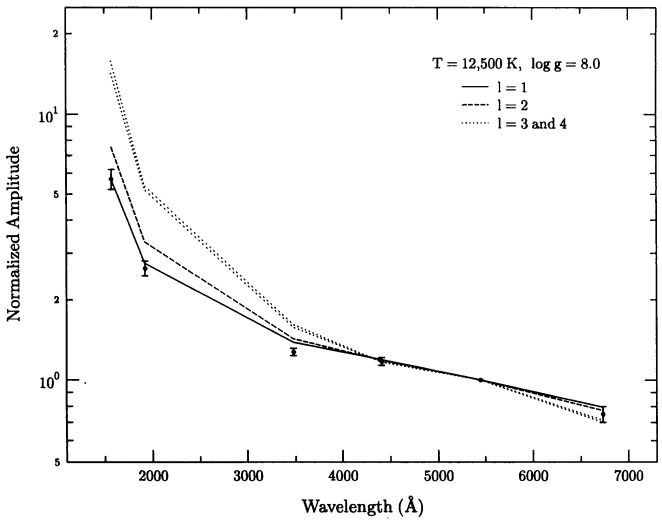

FIG. 7.—Theoretical amplitudes of $\ell = 1$ to $\ell = 4$ nonradial g-mode pulsations in DA white dwarfs averaged over the response functions of the F145M, F184W, U, B, V, and R filters. The amplitudes have been calculated for a model with $T = 12{,}500$ K and $\log g = 8.0$, and have been normalized so that the amplitude through the V filter is 1.0. The observed amplitudes, also normalized, have been superposed on the theoretical amplitudes.

periods as long as 215.2 s. The choice between $\ell = 1$ and $\ell = 2$ must, however, be determined by the goodness of the fits of the models to the data. We will use a Bayesian analysis to quantify the goodness of fit.[7]

For our application Bayes's theorem becomes (see, for example, Schmitt 1969)

$$P(T, g, \ell) \propto P_0(T, g, \ell) L(a, \sigma \mid T, g, l) , \quad (5)$$

where $P_0(T, g, \ell)$ and $P(T, g, \ell)$ are the prior and posterior probability densities for the models with T, g, and ℓ; and $L(a, \sigma \mid T, g, \ell)$ is the likelihood that a model with T, g, and ℓ will give the observed amplitudes and standard deviations. The proportionality constant is determined from the requirement that the sum of all the posterior probabilities equals 1. The likelihood is the product of the likelihoods for the individual filters:

$$L(a, \sigma \mid T, g, \ell) = \prod_i L(a_i, \sigma_i \mid T, g, \ell) . \quad (6)$$

where a_i and σ_i are the amplitude and standard deviation in filter i, and where we assume that the individual likelihoods are given by Gaussian distributions:

$$L(a_i, \sigma_i \mid T, g, \ell) = \frac{1}{(2\pi)^{1/2}\sigma_i} \exp\left\{-\frac{1}{2\sigma_i^2}[a_i - A_i(T, g, \ell)]^2\right\} . \quad (7)$$

The $A_i(T, g, \ell)$ are the theoretical amplitudes in filter i for a model with T, g, and ℓ.

The choice of a prior probability distribution can be an interesting and subtle problem, but in the present application the results are so conclusive that the details of the prior are irrelevant. We will, therefore, simply adopt a flat prior, $P_0(T, g, l) =$ constant, for $\ell = 1$ or 2, and $P_0(T, g, \ell) = 0$ for all other values of ℓ. This choice for the prior is equivalent to assuming that we have no information about T, g, or ℓ except that ℓ must be 1 or 2.

Our first calculation of the posterior probabilities showed that there is a strong correlation between T and $\log g$. Models with $\log g = 7.5$ and $\log g = 8.0$ fit the data almost equally well, but for $\log g = 7.5$ the best model has a temperature near 11,750 K, whereas for $\log g = 8.0$ the best model has a temperature near 12,375 K. Fortunately, we find the same value of ℓ, and with the same high confidence, for all values of $\log g$ in our grid. We will, therefore, present the calculations only for $\log g = 8.0$. As we will show in the next section, this value of $\log g$ is close to the correct value.

The posterior probabilities for $\log g$ fixed at 8.0 and a flat prior are given in Table 5, in which probabilities less than 10^{-10} are listed as 0.00. The marginal probability $P(\ell)$, which is the sum of the probabilities over temperature and is the total probability for each ℓ, is also given in the table. Models with $\ell = 1$ are preferred with an extremely high confidence:

$$\frac{P(l = 1)}{P(l = 2)} = 5 \times 10^7 .$$

Figure 8 compares the observed amplitudes with the theoretical amplitudes for $\ell = 1$ and for three temperatures near the best-fit temperature at $T = 12{,}375$ K, where the amplitudes at $T = 12{,}375$ K were calculated by linearly interpolating between the nearest grid points. The fit is extremely good. Figure 9 compares the observed amplitudes to the theoretical amplitudes for $\ell = 2$ and for three temperatures near the best-fit temperature at $T = 12{,}000$ K. No one temperature fits all the data. The U, B, V, and R filters require a temperature near 12,000 K, whereas the F145M and F184W filters require a temperature near 13,000 K.

These results are insensitive to errors in the observed amplitudes and standard deviations. To investigate the effect of grossly wrong standard deviations, we multiplied the measured values of σ by a factor of 2 and recalculated the posterior probability. The results are given in columns (4) and (5) of Table 5. Models with $\ell = 1$ are still preferred by a factor $P(\ell = 1)/P(\ell = 2) = 104$. To investigate the effect of grossly wrong amplitudes, we excluded each filter individually and recalculated the posterior probability. The $\ell = 1$ models were always strongly preferred, with $P(\ell = 1)/P(\ell = 2) > 10^2$ for all

TABLE 5

PROBABILITIES THAT MODELS WITH T AND ℓ ARE CORRECT FITS TO DATA
(Flat Prior, $\log g = 8.0$)

TEMPERATURE (K) (1)	MEASURED σ		MEASURED $\sigma \times 2$	
	$\ell = 1$ (2)	$\ell = 2$ (3)	$\ell = 1$ (4)	$\ell = 2$ (5)
11,000	0.00	0.00	2.35E−6	0.00
11,250	0.00	0.00	1.90E−9	0.00
11,500	0.00	0.00	0.00	0.00
11.750	0.00	0.00	1.22E−8	0.00
12,000	0.00	0.00	1.54E−3	0.00
12,250	4.61E−1	0.00	4.69E−1	1.09E−4
12,500	5.39E−1	1.91E−8	4.88E−1	6.69E−3
12,750	9.20E−6	0.38E−9	3.13E−2	2.51E−3
13,000	0.00	0.00	9.39E−4	1.75E−4
13,250	0.00	0.00	3.04E−5	6.85E−6
13,500	0.00	0.00	8.48E−7	1.49E−7
Marginal probability	1.00	1.95E−8	0.9905	0.0095

[7] For those unfamiliar with Bayesian techniques, a traditional χ^2 analysis also yields a strong preference for $\ell = 1$ models.

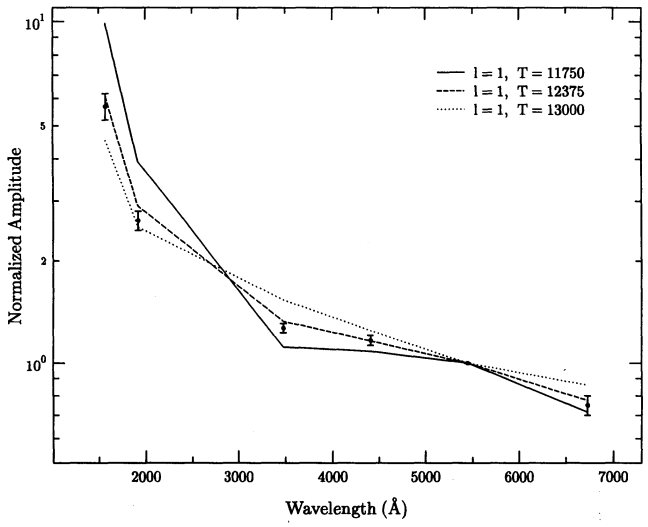

FIG. 8.—Theoretical amplitudes of $\ell = 1$ nonradial g-mode pulsations in DA white dwarfs for the F145M, F184W, U, B, V, and R filters. The amplitudes have been calculated for models with log $g = 8.0$ and for three different temperatures. The amplitudes have been normalized so that the amplitude through the V filter is 1.0. The observed amplitudes, also normalized, have been superposed on the theoretical amplitudes. The theoretical amplitudes for $T = 12{,}375$ K are the best fits to the observed amplitudes.

filters. Thus, the strong preference for the $\ell = 1$ models is highly robust and, moreover, is not dominated by any one filter.

The amplitudes in the *HST* filters were, however, crucial to these results. If we exclude *both* of the *HST* filters from the fit, the preference for the $\ell = 1$ models drops drastically to $P(\ell = 1)/P(\ell = 2) \sim 2$, much too small to allow a reliable determination of ℓ.

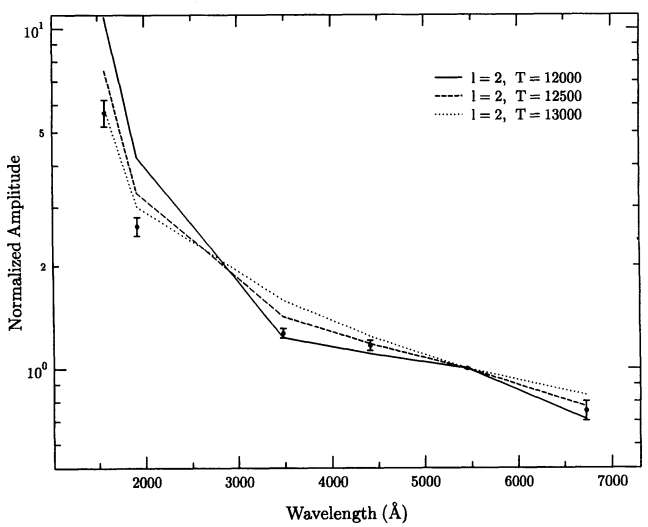

FIG. 9.—Theoretical amplitudes of $\ell = 2$ nonradial g-mode pulsations in DA white dwarfs for the F145M, F184W, U, B, V, and R filters. The amplitudes have been calculated for models with log $g = 8.0$ and for three different temperatures. The amplitudes have been normalized so that the amplitude through the V filter is 1.0. The observed amplitudes, also normalized, have been superposed on the theoretical amplitudes. No one temperature fits all the data for $\ell = 2$: the amplitudes in U, B, V, and R require a temperature near 12,000 K, whereas the amplitudes in the F145M and F184W filters require a temperature near 13,000 K.

5. DISCUSSION

5.1. *The Temperature of G117-B15A*

Although we cannot determine log g and $T_{\rm eff}$ individually from the pulsation data alone, we have found that they are strongly correlated for models that fit the data, such that at log $g = 7.5$ the temperature is 11.750 K and at log $g = 8.0$ the temperature is 12,375 K.

G117-B15A was observed by Daou et al. (1990) as part of an extensive analysis of the optical spectra of the ZZ Ceti stars. They found two possible but disjoint fits of theoretical spectra to the data, one at log $g = 7.81$ and $T = 13{,}200$ K, and the other at log $g = 7.97$ and $T = 12{,}170$ K. They adopted the fit with higher temperature because G117-B15A is among the bluest of the ZZ Ceti stars and should be near the blue edge of the instability strip, and because most of the theoretical computations then available suggested that the blue edge should be near a temperature of 13,000 K. The correlation between log g and T from the pulsation data is inconsistent with and eliminates their high-temperature, low-gravity fit, however. The preferred fit is log $g = 7.97$ and $T = 12{,}170$ K. The standard deviation quoted by Daou et al. (1990) for log g is quite small, ± 0.06, whereas the standard deviation for the temperature is rather large, ± 460 K. We will, therefore, adopt their value for log g, 7.97, but not their value for T, using instead the correlation found from the pulsation data to determine the temperature. Since log $g = 7.97$ is close to log $g = 8.0$, which was used for the fits shown in Table 5 and Figure 8, we simply adopt the best-fit temperature for that gravity: $T_{\rm eff} = 12{,}375$ K.

There are two sources of uncertainty in this temperature: errors in the observational data, and uncertainties in the model atmospheres. Although the preferred value of ℓ did not change when we excluded various filters from the fits described in the last section, the temperature did. The best-fit temperature at log $g = 8.0$ ranged from 12,250 K when the F184W filter was excluded to 12,500 K when the U filter was excluded. We assume that this variation in temperature is a measure of the observational error and adopt half the range of the variation for the uncertainty in the temperature. Thus, the best-fit temperature is $12{,}375 \pm 125$ K. The uncertainty in log g is not a significant contributor to the uncertainty in the temperature.

The temperatures of the ZZ Ceti stars have been measured from *IUE* spectra by Wesemael, Lamontagne, & Fontaine (1986), Lamontagne, Wesemael, & Fontaine (1987), Lamontagne et al. (1989), and most recently by Kepler & Nelan (1993). Kepler & Nelan reanalyzed archival *IUE* spectra of many white dwarfs in and around the ZZ Ceti instability strip. They showed that although the temperatures derived from *IUE* spectra had small formal standard deviations, the external errors due to uncertainties in flux calibrations were large and dominated the error analysis. They found a temperature of $11{,}840 \pm 91$ K for G117-B15A if all the *IUE* and optical data were used, but $13{,}150 \pm 56$ K if only the *IUE* short-wavelength prime (SWP) data were used. Koester & Allard (1993) determined the temperature of G117-B15A from the shape of the *IUE* spectrum near Lyα and its satellite lines, finding 11,860 K, but the quality of the *IUE* spectrum was poor, limiting the reliability of the temperature. The temperature we have derived for G117-B15A is free of calibration errors because we fitted fractional amplitudes, not absolute amplitudes. Thus, we believe that our temperature is much more reliable than those derived from *IUE* spectra.

Bergeron, Wesemael, & Fontaine (1992) have shown that

theoretical spectra of DA white dwarfs with temperatures between ~11,000 and ~13,000 K depend on the convective efficiency adopted for the calculations. The effect is strongest at ultraviolet wavelengths and can change the continuum flux by 25% just below the Balmer jump, but is much less strong at longer wavelengths. The slope of the continuum at longer wavelengths is almost unchanged. Although the temperature determined from direct fits to the continuum flux will certainly depend on the convective efficiency used in the model atmospheres, it is not obvious that fits to the fractional pulsation amplitudes will be similarly affected. We have attempted to estimate the sensitivity of our results to convective efficiency by recalculating the best-fit temperature using only the B, V, and R filters, which cover wavelengths where the convective efficiency is least important. Although using just the B, V, and R filters destroys the sensitivity of the fit to ℓ, it does retain its sensitivity to temperature. The best-fit temperature using these filters is 12,300 K, only slightly different from the temperature using all the filters. We conclude that either the convective efficiency used in our model atmospheres is correct or our method is insensitive to convective efficiency. In either case, the derived temperature, 12,375 ± 125 K, appears to be reliable.

Since G117-B15A is thought to lie close to the blue edge of the ZZ Ceti instability strip, the lower temperature we have derived for it implies a lower temperature for the blue edge. Recent theoretical calculations by Kawaler (1993) and Bradley & Winget (1994) also find a cooler temperature for the blue edge than most previous calculations, although the position of the theoretical blue edge can be moved almost at will by altering the efficiency of convection.

5.2. *The Thickness of the Hydrogen Layer*

The mass of the hydrogen layer is a function of the pulsation period and pulsation indices ℓ and k, and of the mass and effective temperature of the white dwarf. We have deduced $\ell = 1$ and $T = 12{,}375$ K for G117-B15A. From the evolutionary models of Wood (1990), the total mass corresponding to $\log g = 7.97$ is about $0.56\ M_\odot$ for carbon-oxygen white dwarfs, and according to Bradley (1993, 1994) the 215 s pulsation of G117-B15A can only be a $k = 1$ or $k = 2$ mode. Of the models calculated by Bradley (1993, 1994), the one in which the 215 s pulsation is the $\ell = 1$, $k = 2$ mode has a mass and temperature close to those of G117-B15A, $0.55\ M_\odot$ and 12,530 K. The mass of the hydrogen layer in this model is $8 \times 10^{-5}\ M_\odot$. Bradley's model in which the 215 s pulsation is a $k = 1$ mode has a mass too low to match G117-B15A. Instead we use the models calculated by Fontaine et al. (1992). Interpolating in their Figure 1, we find a hydrogen layer mass near $1.0 \times 10^{-6}\ M_\odot$.

While we can expect further fine tuning of the hydrogen layer masses derived from pulsation theory, they probably lie between 1.0×10^{-6} and $8 \times 10^{-5}\ M_\odot$. Although the range of permitted masses is large, covering nearly two orders of magnitude, it is encouraging to note that it does overlap (barely) the range of hydrogen layer masses predicted by Iben & McDonald (1986) from models for the ejection of planetary nebulae, $(8\text{–}13) \times 10^{-5}\ M_\odot$. The agreement would be improved if there is additional mass loss after ejection of the planetary nebula. However, as noted by Fontaine et al. (1994), the mass is too large to be consistent with models that explain the spectral evolution of white dwarfs by invoking a thin layer of hydrogen.

5.3. *The Rate of Change of the* 215 s *Period*

Measurements by Kepler et al. (1991) suggested that the rate of change of the 215 s pulsation period is $\dot{P} = (12.0 \pm 3.5) \times 10^{-15}$ s s^{-1}, and this surprisingly large rate engendered a rash of interpretive papers (e.g., Bradley, Winget, & Wood 1992; Fontaine et al. 1991; Isern, Hernanz, & Garcia-Berro 1992). For a given rate of cooling, the rate of change of a pulsation period depends on ℓ and k. All these papers dealt with the problem of unknown pulsation indices by taking an average of the rates of period change for a large number of pulsation modes with periods near 215 s, typically averaging over $\ell = 1$, 2, and 3. This is an unsatisfactory procedure because the rates of period change for different values of ℓ can differ by a factor of 2 or more, vitiating any strong conclusions that might be derived from a measurement of $\dot{P}$. The immediacy of these efforts has subsided now that additional observations of G117-B15A have shown that $\dot{P}$ is much smaller, $(3.2 \pm 2.8) \times 10^{-15}$ s s^{-1} (Kepler 1993). We note, however, that the rates of change of period are larger for smaller values of ℓ (Bradley et al. 1992), and since $\ell = 1$ for the 215 s pulsation, a true measurement of $\dot{P}$ may still be within reach.

5.4. *Summary*

We have measured the photometric amplitude of the 215 s pulsation of G117-B15A in six passbands with effective wavelengths from 1570 to 6730 Å, and we have shown that the index of the pulsation is $\ell = 1$ with a high degree of confidence. Combining our results with earlier results by Daou et al. (1990), we find that the temperature and gravity of G117-B15A are $T = 12{,}375 \pm 125$ K and $\log g = 7.97$. Since G117-B15A is thought to lie close to the blue edge of the instability strip, this low temperature implies a low temperature for the blue edge. The mass of the hydrogen layer in G117-B15A lies between 1.0×10^{-6} and $8 \times 10^{-5}\ M_\odot$. This range of masses is consistent with the masses predicted by models for the ejection of planetary nebulae, $(8\text{–}13) \times 10^{-5}\ M_\odot$. The mass is too large to be consistent with the existing models invoking thin hydrogen layers to explain the spectral evolution of white dwarfs.

We thank P. A. Bradley and G. Fontaine for discussions on the theory of pulsating and nonpulsating white dwarfs, T. F. Ramseyer for calculating the response functions of the two high-speed photometers, and W. H. Jefferys for discussions on Bayesian statistics. This work was supported in part by HSP GTO grant NASG5-1613.

REFERENCES

Bergeron, P., Wesemael, F., & Fontaine, G. 1992, ApJ, 387, 288
Bless, R. C., et al. 1994, AJ, in preparation
Bradley, P. A. 1993, Ph.D. thesis, Univ. Texas at Austin
———. 1994, ApJ, submitted
Bradley, P. A., & Winget, D. E. 1994, ApJ, 421, 236
Bradley, P. A., Winget, D. E., & Wood, M. A. 1992, ApJ, 391, L33
Brassard, P., Fontaine, G., Wesemael, F., & Talon, A. 1993, in White Dwarfs: Advances in Observation and Theory, ed. M. A. Barstow (Dordrecht: Kluwer), 485
Brassard, P., Wesemael, F., & Fontaine, G. 1987, in IAU Colloq. 95, Second Conference on Faint Blue Stars, ed. A. G. D. Phillip, D. S. Hayes, & J. Liebert (Schenectady: Davis), 669
Clemens, J. C. 1993, Ph.D. thesis, Univ. Texas at Austin
D'Antona, F., & Mazzitelli, I. 1991, in IAU Symp. 145, The Photospheric Abundance Connection, ed. G. Michaud & A. Tutukov (Dordrecht: Reidel), 399
Daou, D., Wesemael, F., Bergeron, P., Fontaine, G., & Holberg, J. B. 1990, ApJ, 364, 242

Fontaine, G., & Brassard, P. 1994, in Stellar and Circumstellar Astrophysics, ed. G. Wallerstein (San Francisco: ASP), in press
Fontaine, G., Brassard, P., Bergeron, P., & Wesemael, F. 1992, ApJ, 399, L91
Fontaine, G., Brassard, P., Wesemael, F., Kepler, S. O., & Wood, M. A. 1991, in White Dwarfs, ed. G. Vauclair & E. Sion (Dordrecht: Kluwer), 153
Fontaine, G., Brassard, P., Wesemael, F., & Tassoul, M. 1994, ApJ, in press
Fontaine, G., & Wesemael, F. 1991, in IAU Symp. 145, Evolution of Stars: The Photospheric Abundance Connection, ed. G. Michaud & A. Tutukov (Dordrecht: Reidel), 421
Iben, I., & MacDonald, J. 1986, ApJ, 301, 164
Isern, J., Hernanz, M., & Garcia-Berro, E. 1992, ApJ, 392, L23
Jordan, S., & Koester, D. 1986, A&AS, 65, 367
Kawaler, S. D. 1993, ApJ, 404, 294
Kawaler, S. D., & Bradley, P. A. 1994, ApJ, 427, 415
Kawaler, S. D., & Hansen, C. J. 1989, in IAU Colloq. 114, White Dwarfs, ed. G. Wegner (Berlin: Springer), 97
Kepler, S. O. 1993, Baltic Astron., 2, 444
Kepler, S. O., & Nelan, E. P. 1993, AJ, 105, 608
Kepler, S. O., Robinson, E. L., Nather, R. E., & McGraw, J. T. 1982, ApJ, 254, 676
Kepler, S. O., et al. 1991, ApJ, 378, L45
Koester, D., & Allard, N. 1993, in White Dwarfs: Advances in Observation and Theory, ed. M. A. Barstow (Dordrecht: Kluwer), 237
Koester, D., Schulz, H., & Weidemann, V. 1979, A&A, 76, 262
Lamontagne, R., Wesemael, F., & Fontaine, G. 1987, in IAU Colloq. 95, Second Conf. on Faint Blue Stars, ed. A. G. Davis Phillip, D. S. Hayes, & J. Liebert (Schenectady: Davis), 677
Lamontagne, R., Wesemael, F., Fontaine, G., Wegner, G, & Nelan, E. P. 1989, in IAU Colloq. 114, White Dwarfs, ed. G. Wegner (New York: Springer), 109
McGraw, J. T., & Robinson, E. L. 1976, ApJ, 205, L155
Robinson, E. L., Kepler, S. O., & Nather, R. E. 1982, ApJ, 259, 219 (RKN)
Schmitt, S. A. 1969, Measuring Uncertainty, An Elementary Introduction to Bayesian Statistics (Reading: Addison-Wesley)
Wesemael, F., Lamontagne, R., & Fontaine, G. 1986, AJ, 91, 1376
Winget, D. E. 1988, in IAU Symp. 123, Advances in Helio- and Asteroseismology, ed. J. Christensen-Dalsgaard & S. Frandsen (Dordrecht: Reidel), 305
Winget, D. E., et al. 1994, ApJ, in press
Wood, M. A. 1990, Ph.D. thesis, Univ. Texas at Austin
———. 1992, ApJ, 386, 539
Zhang, E., Robinson, E. L., Ramseyer, T. F., Shetrone, M. D., & Stiening, R. F. 1991, ApJ, 381, 534